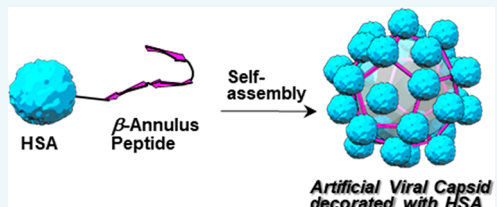


## Artificial Viral Capsid Dressed Up with Human Serum Albumin

Kazunori Matsuura<sup>\*†‡</sup> and Takahide Honjo<sup>†</sup>

<sup>†</sup>Department of Chemistry and Biotechnology, Graduate School of Engineering, and <sup>‡</sup>Centre for Research on Green Sustainable Chemistry, Tottori University, 4-101 Koyama-Minami, Tottori 680-8552, Japan

**ABSTRACT:** Capsid of tomato bushy stunt virus consists of an outer coat protein shell decorated on an internal skeleton comprising a  $\beta$ -annulus motif. We mimicked this capsid structure with our artificial viral capsid dressed up with protein. We synthesized the  $\beta$ -annulus peptide bearing a Cys at the C-terminal side and linked it with Cys34 of the human serum albumin (HSA) via a bismaleimide linker. The  $\beta$ -annulus peptide-HSA conjugate self-assembled into spherical structures of a 50–70 nm size range in the Tris-HCl buffer, with the  $\zeta$ -potential of assemblies of such conjugate revealing that HSA proteins were displayed on the outer surface of the artificial viral capsid. Interestingly, the critical aggregation concentration (CAC) of the conjugate in the Tris-HCl buffer at 25 °C was approximately 0.01  $\mu$ M, or 1/2500 lower than that of the unmodified  $\beta$ -annulus peptides, suggesting that the artificial viral capsids were stabilized via HSA modification. The present strategy of constructing protein nanocapsule by self-assembly of a  $\beta$ -annulus peptide–protein conjugate is simpler than that of previously reported protein nanocapsules.



Natural spherical viruses comprise genome nucleic acids encapsulated in protein assembly with icosahedral symmetry called capsids, which are regularly self-assembled from multiples of 60 protein subunits.<sup>1</sup> With viral capsids being recognized as bionanomaterials possessing discrete size and constant aggregation number, natural viral capsids and virus-like proteinous capsids have been utilized as nanocarriers and nanoreactors.<sup>2–7</sup> For application as drug delivery carriers, encapsulation of anticancer drugs and protein drugs into spherical viral capsids and surface decoration of capsids with cell-targeting ligands have been reported.<sup>8–14</sup> However, the potential toxicity of natural viral capsids is often hampered for their application as drug-carriers. If an artificial nanocapsule decorated with any proteins can be constructed by self-assembly, then protein nanocapsules would be promising candidates as less toxic designer drug carriers.

To date, nanoarchitecture assemblies from rationally designed peptides<sup>15–26</sup> and proteins<sup>15,20,27–37</sup> have been progressively developed. Nolte et al. reported that a giant amphiphile reconstructed from an apo-horseradish peroxidase and heme-modified polystyrene self-assembled into protein vesicle.<sup>32,33</sup> Yeates et al. demonstrated that fusion proteins comprising trimer-forming and dimer-forming units self-assembled into tetrahedral and cubic protein assemblies.<sup>34,35</sup> Recently, Baker et al. developed a computationally designed icosahedral nanocage that self-assembles from trimeric protein building blocks.<sup>36</sup> Kawakami et al. developed a polyhedral protein cage that self-assembled from fusion proteins consisting of pentamer-forming and dimer-forming coiled-coil units.<sup>37</sup> Although such recent development of discrete protein assemblies, rationally designing artificial nanocapsules decorated with any proteins at the surface remains challenging.

Capsid of tomato bushy stunt virus (TBSV) is formed by the self-assembly of 180 quasi-equivalent protein subunits

containing 388 amino acids, in which the  $\beta$ -annulus motif participates in the formation of a dodecahedral internal skeleton.<sup>38–40</sup> We have demonstrated that 24-mer  $\beta$ -annulus peptides (INHVGTTGGAIMAPVAVTRQLVGS) of TBSV spontaneously self-assembled into a hollow peptide nanocapsule (artificial viral capsid) within a size range of 30–50 nm in water (Figure 1A).<sup>20,41,42</sup> The artificial viral capsid can encapsulate anionic dyes, DNA, quantum dots, and His-tagged proteins in the cationic interior.<sup>43–47</sup> Natural TBSV capsid structure can be regarded where the outer coat protein shell is decorated on the internal skeleton consisting of a  $\beta$ -annulus motif. Therefore, even if the coat proteins are replaced with other proteins, we envisage that artificial viral capsids would be constructed by the self-assembly of  $\beta$ -annulus peptide connected with proteins. The pH dependence of the  $\zeta$ -potential of artificial viral capsids indicates that the C-terminals of  $\beta$ -annulus peptides are exposed to the outer surface.<sup>43</sup> These properties enabled surface modification of artificial viral capsids with gold nanoparticles,<sup>48</sup> coiled-coil peptides,<sup>49</sup> and single-strand DNAs<sup>50</sup> by C-terminal modification of the  $\beta$ -annulus peptide. In this study, we describe the construction of an artificial viral capsid dressed-up with human serum albumin (HSA) at the outer surface, which is comparable in that coat proteins of TBSV are replaced with HSA. As HSA is a blood-compatible protein and is not immunogenic,<sup>51–53</sup> an HSA-decorated artificial viral capsid can potentially be applied as a biocompatible material.

Received: May 6, 2019

Revised: May 25, 2019

Published: June 3, 2019

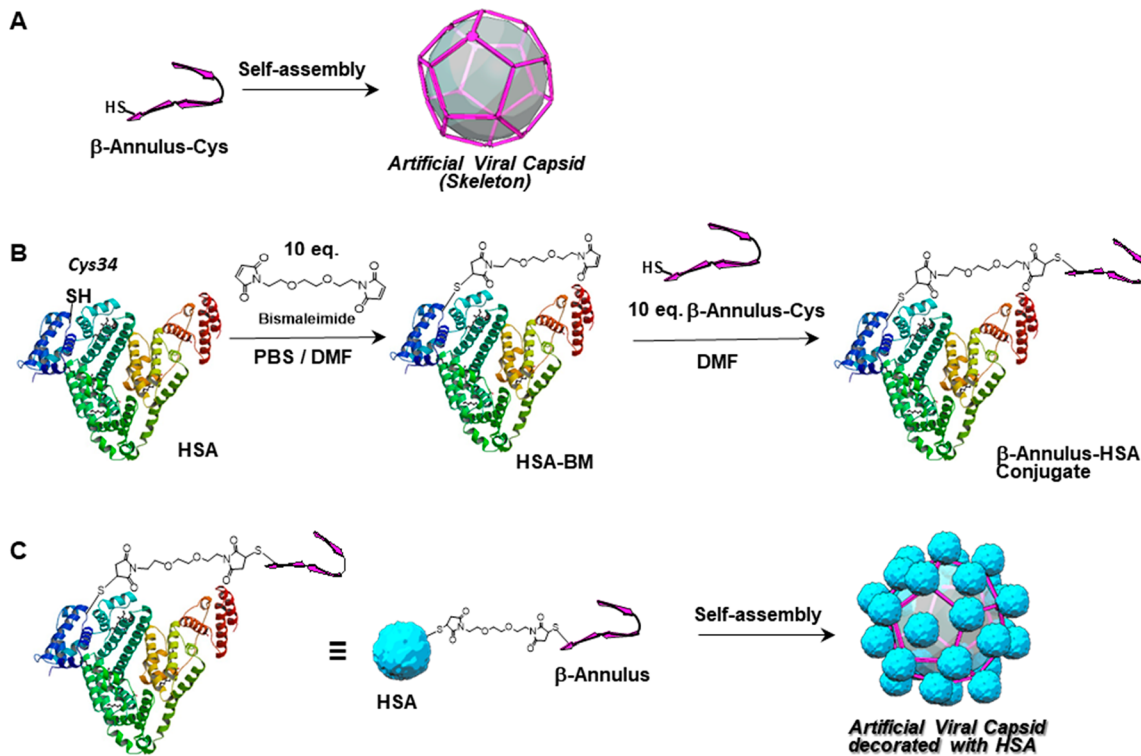


**Figure 1.** Schematic illustration of (A) the self-assembly of unmodified artificial viral capsid, (B) the preparation of  $\beta$ -annulus peptide–HSA conjugate, and (C) the self-assembly of artificial viral capsid decorated with HSA.

## ■ RESULTS AND DISCUSSION

**Synthesis of  $\beta$ -Annulus Peptide–HSA Conjugate.** HSA (66.4 kDa) is known to contain only one reduced Cys at 34-position.<sup>51,52</sup> We designed a  $\beta$ -annulus peptide–HSA conjugate, linked between Cys34 of HSA and Cys of  $\beta$ -annulus peptide at the C-terminal side via a bismaleimide linker (Figure 1B). As the C-terminal of  $\beta$ -annulus peptide can be directed to the outer surface of an artificial viral capsid,<sup>43</sup> we estimated that HSA would be displayed on the capsid surface by self-assembly of the conjugates (Figure 1C). We synthesized the 24-mer  $\beta$ -annulus peptide bearing Cys at the C-terminal side ( $\beta$ -annulus-Cys peptide: INHVGGTGGAIMAPVAVTRQL-VCS) by a standard solid-phase Fmoc-chemistry, purified it by reverse-phase HPLC, and confirmed it by MALDI-TOF-MS ( $m/z = 2351$ ). Cys34 of HSA reacted with excess amount of bismaleimide linker (1,8-bismaleimide diethylene glycol) in phosphate buffered saline PBS (pH 7.4) to obtain a HSA–BM conjugate. Another maleimide of this conjugate was allowed to react with  $\beta$ -annulus-Cys peptide in DMF, and then the excess peptide was removed by dialysis to isolate a  $\beta$ -annulus-HSA conjugate. There was hardly a reaction between HSA–BM and  $\beta$ -annulus-Cys peptide in the aqueous or acetonitrile solution, probably due to poor solubility of  $\beta$ -annulus peptide in these solvents. MALDI-TOF-MS of the obtained  $\beta$ -annulus peptide–HSA conjugate showed a broad peak at  $m/z = 69\,255$ , which corresponds to the molecular weight of HSA added one  $\beta$ -annulus peptide chain. We conducted a quantitative analysis of thiol groups using Ellman method, which revealed that thiol groups of almost all HSA were consumed by linking with  $\beta$ -annulus peptide. These results indicate the successful synthesis of the  $\beta$ -annulus peptide–HSA conjugate.

**Self-Assembling Behavior of  $\beta$ -Annulus Peptide–HSA Conjugate.** The average diameter obtained from dynamic

light scattering (DLS) measurement of the  $\beta$ -annulus peptide–HSA conjugate solution at  $0.1\ \mu\text{M}$  in 10 mM Tris-HCl buffer (pH 7.0) showed the formation of assemblies with the size of  $54 \pm 13\ \text{nm}$  and  $141 \pm 60\ \text{nm}$  (Figure 2A). A TEM image of the aqueous solution of the conjugate at the same concentration shows the abundance of spherical structures with sizes ranging from 50 to 70 nm (Figure 2D), which are slightly larger than those of the self-assembled artificial viral capsid from the unmodified  $\beta$ -annulus peptide ( $48 \pm 13\ \text{nm}$ ).<sup>41</sup> This indicates that HSA modification at the C-terminal of the  $\beta$ -annulus peptide had minimal influence on the self-assembling behavior. Considering size of HSA (about 5 nm), the increase of size by HSA modification on artificial viral capsid seems to be appropriate. DLS-observed assemblies larger than 100 nm might be caused by the secondary aggregation of capsid-like spherical assemblies. On the contrary, both DLS and TEM showed that intact HSA did not self-assemble at  $0.1\ \mu\text{M}$  (Figure 2B,E). Although the unmodified  $\beta$ -annulus-Cys peptide self-assembled into spherical structures with the size of roughly 50 nm above critical aggregation concentration ( $\text{CAC} = 25\ \mu\text{M}$ ), such assemblies were not observed at  $0.1\ \mu\text{M}$  (Figure 2C,F), indicating the interesting feature of the  $\beta$ -annulus peptide–HSA conjugate self-assembling into spherical structures, but not its constituents (HSA and  $\beta$ -annulus-Cys peptide), at  $0.1\ \mu\text{M}$ .

**Characterization of HSA-Decorated Artificial Viral Capsid.** Figure 3A,B shows the  $\beta$ -annulus peptide–HSA conjugate self-assembling into spherical artificial viral capsids of sizes 50–100 nm, over a wide concentration range ( $0.01$ – $10\ \mu\text{M}$ ). The conjugate concentration dependence on the scattering intensity obtained from DLS measurements revealed that the CAC of the conjugate in Tris-HCl buffer at  $25\ ^\circ\text{C}$  was approximately  $0.01\ \mu\text{M}$  (Figure 3D). In fact, the conjugate formed spherical capsid structures of  $84 \pm 26\ \text{nm}$  size even at

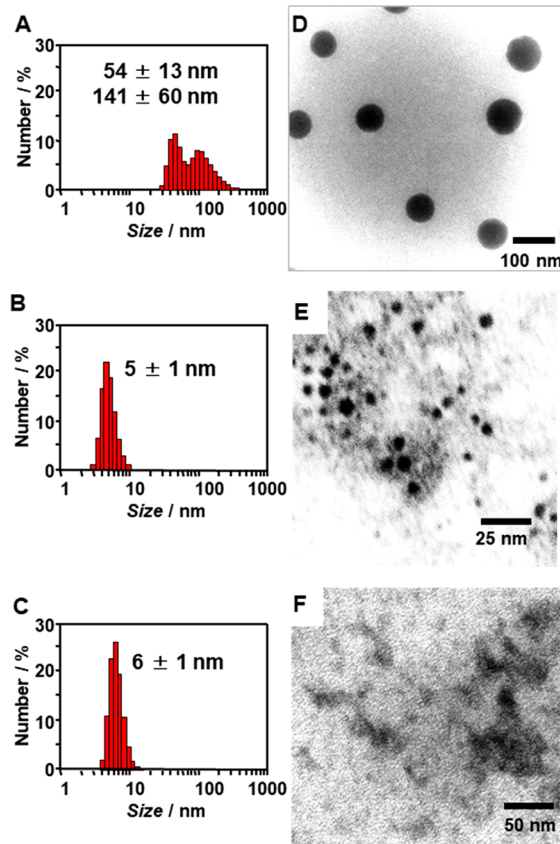


**Figure 2.** Size distributions obtained from DLS (A–C) and TEM images (D–F) for solutions of 0.1  $\mu\text{M}$   $\beta$ -annulus peptide–HSA conjugate (A, D), 0.1  $\mu\text{M}$  HSA (B, E), and 0.1  $\mu\text{M}$   $\beta$ -annulus–Cys peptide in 10-mM Tris–HCl buffer (pH 7.0) at 25 °C. TEM samples were stained with sodium phosphotungstate.

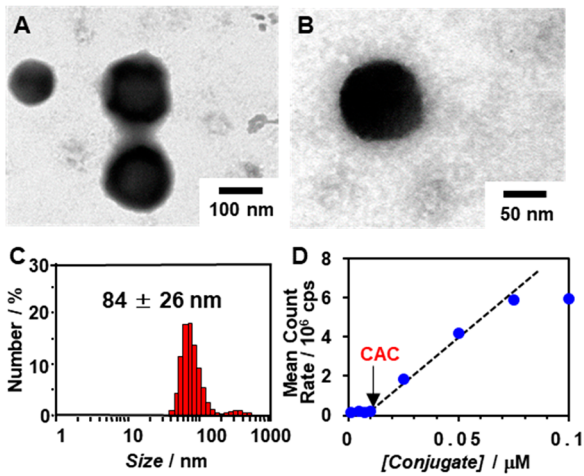


**Figure 3.** (A,B) TEM images of  $\beta$ -annulus peptide–HSA conjugate at 10  $\mu\text{M}$  (A) and 0.01  $\mu\text{M}$  (B) in 10 mM Tris–HCl buffer (pH 7.0). (C) Size distribution obtained from DLS for the solution of the 0.01  $\mu\text{M}$  conjugate in 10 mM Tris–HCl buffer (pH 7.0) at 25 °C. (D) Effect of concentration of the conjugate on scattering intensity, as determined by DLS at 25 °C.

0.01  $\mu\text{M}$  (Figure 3C). Interestingly, the  $\beta$ -annulus peptide–HSA conjugate can self-assemble at 1/2500 lower concentration than CAC (25  $\mu\text{M}$ ) of the unmodified  $\beta$ -annulus peptides,<sup>41</sup> suggesting that artificial viral capsids were stabilized

by modification with HSA, probably due to lateral interactions between dense HSAs on the capsid and interactions between HSA and the capsid surface.

To confirm that HSAs were displayed on the outer surface of the artificial viral capsids, we measured the  $\zeta$ -potential of the  $\beta$ -annulus peptide–HSA conjugate assemblies. The known isoelectric point (*pI*) of HSA is 4.8. The  $\zeta$ -potential of the assemblies was  $-43 \pm 15$  mV at pH 7.0, whereas those at pH 3.5 and 4.8 (*pI*) were  $+14 \pm 7$  mV and approximately neutral ( $-4.4 \pm 5$  mV), respectively (Figure 4A). On the contrary, the

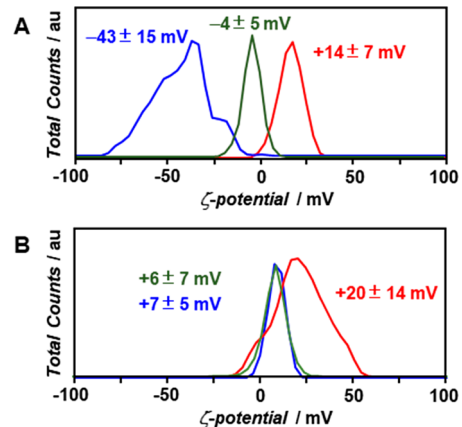


**Figure 4.**  $\zeta$ -Potentials of the assemblies of (A) the  $\beta$ -annulus peptide–HSA conjugate (0.1  $\mu\text{M}$ ) and (B) the  $\beta$ -annulus–Cys peptide (0.1 mM) in water at pH 3.5 (red), 4.8 (green), and 7.0 (blue).

$\zeta$ -potentials of the unmodified artificial viral capsids were almost neutral at pH 7.0 and 4.8, respectively (Figure 4B). The negative charges on the assemblies of the conjugate at pH 7 might be caused by the presence of HSA on the surface. Therefore, these results indicate that HSA proteins were displayed on the outer surface of the artificial viral capsid.

## CONCLUSION

We have demonstrated that the  $\beta$ -annulus peptide conjugate linking HSA via the bismaleimide linker at the C-terminal self-assembled into the artificial viral capsid of sizes within 50–100 nm dressed up with HSA. Surprisingly, the HSA-decorated artificial viral capsid was formed even at very low concentration, 0.01  $\mu\text{M}$ . Given that HSA is abundant protein in human blood plasma, the HSA-decorated artificial viral capsid can be potentially a drug delivery carrier bearing no toxicity and immunoresponse, because artificial viral capsids self-assembled from  $\beta$ -annulus peptide can encapsulate various guest molecules.<sup>20,43–47</sup> The present strategy of fabricating a protein nanocapsule by the self-assembly of a  $\beta$ -annulus peptide–protein conjugate is simpler than that of previously reported protein nanocapsules which were constructed from fusion proteins bearing symmetric subunits.<sup>34–37</sup> Using this versatile strategy, we envisage to fabricate artificial viral capsids dressed up with various functional proteins, such as enzymes and receptors.

## EXPERIMENTAL PROCEDURES

**General.** Reagents were obtained from commercial sources and were used without further purification. Deionized water of high resistivity (>18 MΩ cm) was purified using a Millipore Purification System (Milli-Q water) and was used as

a solvent for the present peptides. Reversed-phase HPLC was performed at ambient temperature using a Shimadzu LC-6AD liquid chromatograph equipped with a UV/vis detector (220 nm, Shimadzu SPD-10AVvp) and Inertsil WP300 C18 (GL Science) columns (250 × 4.6 mm or 250 × 20 mm). MALDI-TOF mass spectra were obtained using an Autoflex III instrument (Bruker Daltonics) in linear/positive mode with  $\alpha$ -cyano-4-hydroxy cinnamic acid ( $\alpha$ -CHCA) or sinapinic acid as a matrix. CD spectra were taken at 25 °C in a 1.0 mm quartz cell using a JASCO J-820 spectrophotometer equipped with a Peltier-type thermostatic cell holder.

**Synthesis of  $\beta$ -Annulus-Cys Peptide.** The peptide H-Ile-Asn(Trt)-His(Trt)-Val-Gly-Gly-Thr(tBu)-Ile-Met-Ala-Pro-Val-Ala-Val-Thr(tBu)-Arg(Mtr)-Gln(Trt)-Leu-Val-Cys(Trt)-Ser(tBu)-Alko-PEG resin was synthesized on Fmoc-Ser(tBu)-Alko-PEG resin (521 mg, 0.21 mmol/g; Watanabe Chemical Ind. Ltd.) using Fmoc-based coupling reactions (4 equiv of Fmoc amino acids). A N-methylpyrrolidone (NMP) solution containing (1-cyano-2-ethoxy-2-oxoethylidenaminoxy) dimethylamino-morpholino-carbenium hexafluorophosphate (COMU) and diisopropylamine was used as the coupling reagent. Fmoc deprotection was achieved using 20% piperidine in *N,N*-dimethylformamide (DMF). Progression of the coupling reaction and Fmoc deprotection was confirmed by TNBS and chloranil test kit (Tokyo Chemical Industry Co., Ltd.). Peptidyl-resins were washed with NMP and were then dried under a vacuum. Peptides were deprotected and cleaved from the resin by treatment with a cocktail of trifluoroacetic acid (TFA)/1,2-ethanedithiol/triisopropylsilane/thioanisole/water = 8.25/0.25/0.1/0.5/0.5 (mL) at room temperature for 4 h. Reaction mixtures were filtered to remove resins, and filtrates were concentrated under a vacuum. The peptide was precipitated by adding methyl *tert*-butyl ether (MTBE) to the residue and the supernatant was decanted. After three times of repetitive washing with MTBE, the precipitated peptide was dried *in vacuo*. The crude product was purified by reverse-phase HPLC eluting with a linear gradient of CH<sub>3</sub>CN/water containing 0.1% TFA (20/80 to 80/20 over 100 min). The fraction containing the desired peptide was lyophilized to give 23.3 mg of a flocculent solid (7.9% yield). MALDI-TOF MS (matrix:  $\alpha$ -CHCA): *m/z* = 2351 [M]<sup>+</sup>.

**Synthesis of  $\beta$ -Annulus Peptide–HSA Conjugate.** HSA (13.2 mg, 0.2  $\mu$ mol, Sigma) was dissolved in 1.0 mL of 1× phosphate buffered saline (1× PBS, pH7.4). The aqueous solution (1.0 mL) of HSA in PBS was mixed with 0.1 M solution (20  $\mu$ L) of 1,8-bismaleimide diethylene glycol (BM(PEG)<sub>2</sub>, Thermo) in DMF. The mixture was stirred at room temperature for 3 h, and then dialyzed in water with a dialysis membrane (Mini Dialysis kit 8 kDa cutoff, GE Healthcare) for 12 h to remove excess BM(PEG)<sub>2</sub>. The obtained HSA–BM conjugate was lyophilized without further purification for next reaction. The powder of HSA–BM conjugate was mixed with a DMF solution (1.0 mL) of  $\beta$ -annulus-Cys peptide. The mixture was stirred at room temperature for 5 h, and then dialyzed in water using Mini Dialysis kit 8 kDa cutoff (GE Healthcare) for 12 h. The internal solution was lyophilized to give a colorless flocculent solid. The yield was 91%. MALDI-TOF MS (matrix:sinapinic acid): *m/z* = 69 255.

**Dynamic Light Scattering and  $\zeta$ -Potential.** Stock solutions (0.1 mM) of  $\beta$ -annulus peptide–HSA conjugate in 10 mM Tris-HCl buffer (pH 7.0) were prepared by dissolving in buffer with sonication for 5 min. The samples were prepared

by diluting the stock solutions with 10 mM Tris-HCl buffer (pH 7.0) and were incubated at 25 °C for 1 h before DLS measurements using a Zetasizer Nano ZS (MALVERN) instrument at 25 °C with an incident He–Ne laser (633 nm). During measurements, count rates (sample scattering intensities) were also provided. Correlation times of the scattered light intensities  $G(\tau)$  were measured several times and there means were calculated for the diffusion coefficient. Hydrodynamic diameters of the scattering particles were calculated using the Stokes–Einstein equation. Zeta potentials of the  $\beta$ -annulus peptide–HSA conjugate at pH 3.5, 4.8, and 7.0 were measured at 25 °C using a Zetasizer Nano ZS (MALVERN) with a DT1061 clear disposable zeta cell.

**Transmission Electron Microscopy.** Aliquots (5  $\mu$ L) of the DLS samples were applied to hydrophilized carbon-coated Cu-grids (C-SMART Hydrophilic TEM grids, ALLANCE Biosystems) for 1 min and were then removed. Subsequently, the TEM grids were instilled in the staining solution, 2% phosphotungstic acid (Na<sub>3</sub>(PW<sub>12</sub>O<sub>40</sub>) (H<sub>2</sub>O)<sub>n</sub>) aqueous solution (5  $\mu$ L), for 1 min, and then removed. After the sample-loaded carbon-coated grids were dried in *vacuo*, they were observed by TEM (JEOL JEM 1400 Plus), using an accelerating voltage of 80 kV.

## ■ AUTHOR INFORMATION

### Corresponding Author

\*E-mail: [ma2ra-k@tottori-u.ac.jp](mailto:ma2ra-k@tottori-u.ac.jp). Telephone: +81 857-31-5262.

### ORCID

Kazunori Matsuura: [0000-0001-5472-7860](http://orcid.org/0000-0001-5472-7860)

### Notes

The authors declare no competing financial interest.

## ■ ACKNOWLEDGMENTS

This research was partially supported by The Asahi Glass Foundation and a Grant-in-Aid for Scientific Research on Innovative Areas “Chemistry for Multimolecular Crowding Biosystems” (JSPS KAKENHI Grant No. JP18H04558).

## ■ REFERENCES

- (1) Tars, K. (2016) in *Viral Nanotechnology* (Khudyakov, Y., and Pumpsens, P., Eds.) Chapter 1, CRC Press.
- (2) Douglas, T., and Young, M. (2006) Viruses: Making friends with old foes. *Science* 312, 873–875.
- (3) Steinmetz, N. F., and Evans, D. J. (2007) Utilisation of plant viruses in bionanotechnology. *Org. Biomol. Chem.* 5, 2891–2902.
- (4) Parapostolou, D., and Howorka, S. (2009) Engineering and exploiting protein assemblies in synthetic biology. *Mol. BioSyst.* 5, 723–732.
- (5) Witus, L. S., and Francis, M. B. (2011) Using synthetically modified proteins to make new materials. *Acc. Chem. Res.* 44, 774–783.
- (6) Bronstein, L. M. (2011) Virus-based nanoparticles with inorganic cargo: What does the future hold? *Small* 7, 1609–1618.
- (7) Azuma, Y., Edwardson, T. G. W., and Hilvert, D. (2018) Tailoring lumazine synthase assemblies for bionanotechnology. *Chem. Soc. Rev.* 47, 3543–3557.
- (8) van Rijn, P., and Schirhagl, R. (2016) Viruses, artificial viruses and virus-based structures for biomedical applications. *Adv. Healthcare Mater.* 5, 1386–1400.
- (9) Rohovie, M. J., Nagasawa, M., and Swartz, J. R. (2017) Virus-like particles: Next-generation nanoparticles for targeted therapeutic delivery. *Bioeng. Transl. Med.* 2, 43–57.

- (10) Ren, Y., Wong, S. M., and Lim, L. Y. (2007) Folic acid-conjugated protein cages of a plant virus: A novel delivery platform for doxorubicin. *Bioconjugate Chem.* **18**, 836–843.
- (11) Tong, G. J., Hsiao, S. C., Carrico, Z. M., and Francis, M. B. (2009) Viral capsid DNA aptamer conjugates as multivalent cell-targeting vehicles. *J. Am. Chem. Soc.* **131**, 11174–11178.
- (12) Min, J., Moon, H., Yang, H. J., Shin, H.-H., Hong, S. Y., and Kang, S. (2014) Development of P22 viral capsid nanocomposites as anti-cancer drug, Bortezomib (BTZ), delivery nanoplatforms. *Macromol. Biosci.* **14**, 557–564.
- (13) Ashley, C. E., Carnes, E. C., Phillips, G. K., Durfee, P. N., Buley, M. D., Lino, C. A., Padilla, D. P., Phillips, B., Carter, M. B., Willman, C. L., et al. (2011) Cell-specific delivery of diverse cargos by bacteriophage MS2 virus-like particles. *ACS Nano* **5**, 5729–5745.
- (14) Schwarz, B., Madden, P., Avera, J., Gordon, B., Larson, K., Miettinen, H. M., Uchida, M., LaFrance, B., Basu, G., Rynda-Apple, A., et al. (2015) Symmetry controlled, genetic presentation of bioactive proteins on the P22 virus-like particle using an external decoration protein. *ACS Nano* **9**, 9134–9147.
- (15) Matsuura, K. (2014) Rational design of self-assembled proteins and peptides for nano- and micro-sized architectures. *RSC Adv.* **4**, 2942–2953.
- (16) Ramakers, B. E. I., van Hest, J. C. M., and Löwik, D. W. P. M. (2014) Molecular tools for the construction of peptide-based materials. *Chem. Soc. Rev.* **43**, 2743–2756.
- (17) de Santis, E., and Ryadnov, M. G. (2015) Peptide self-assembly for nanomaterials: the old new kid on the block. *Chem. Soc. Rev.* **44**, 8288–8300.
- (18) Matsuura, K. (2017) Construction of functional biomaterials by biomolecular self-assembly. *Bull. Chem. Soc. Jpn.* **90**, 873–884.
- (19) Raymond, D. M., and Nilsson, B. L. (2018) Multicomponent peptide assemblies. *Chem. Soc. Rev.* **47**, 3659–3720.
- (20) Matsuura, K. (2018) Synthetic approaches to construct viral capsid-like spherical nanomaterials. *Chem. Commun.* **54**, 8944–8959.
- (21) Inaba, H., and Matsuura, K. (2019) Peptide Nanomaterials Designed from Natural Supramolecular Systems. *Chem. Rec.* **19**, 843.
- (22) Lou, S., Wang, X., Yu, Z., and Shi, L. (2019) Peptide tectonics: Encoded structural complementarity dictates programmable self-assembly. *Adv. Sci.* **6**, 1802043.
- (23) Fletcher, J. M., Harniman, R. L., Barnes, Fr. R. H., Boyle, A. L., Collins, A., Mantell, J., Sharp, T. H., Antognozzi, M., Booth, P. J., Linden, N., et al. (2013) Self-assembling cages from coiled-coil peptide modules. *Science* **340**, 595–599.
- (24) Mosayebi, M., Shoemark, D. K., Fletcher, J. M., Sessions, R. B., Linden, N., Woolfson, D. N., and Liverpool, T. B. (2017) Beyond icosahedral symmetry in packings of proteins in spherical shells. *Proc. Natl. Acad. Sci. U. S. A.* **114**, 9014–9019.
- (25) Ross, J. F., Bridges, A., Fletcher, J. M., Shoemark, D., Alibhai, D., Bray, H. E. V., Beesley, J. L., Dawson, W. M., Hodgson, L. R., Mantell, J., et al. (2017) Decorating self-assembled peptide cages with proteins. *ACS Nano* **11**, 7901–7914.
- (26) Kobayashi, N., Yanase, K., Sato, T., Unzai, S., Hecht, M. H., and Arai, R. (2015) Self-assembling nano-architectures created from a protein nano-building block using an intermolecularly folded dimeric de Novo protein. *J. Am. Chem. Soc.* **137**, 11285–11293.
- (27) Yang, L., Liu, A., Cao, S., Putri, R. M., Jonkheijm, P., and Cornelissen, J. J. L. M. (2016) Self-assembly of proteins: Towards supramolecular materials. *Chem. - Eur. J.* **22**, 15570–15582.
- (28) Luo, Q., Hou, C., Bai, Y., Wang, R., and Liu, J. (2016) Protein assembly: Versatile approaches to construct highly ordered nanostructures. *Chem. Rev.* **116**, 13571–13632.
- (29) Sun, H., Luo, Q., Hou, C., and Liu, J. (2017) Nanostructures based on protein self-assembly: From hierarchical construction to bioinspired materials. *Nano Today* **14**, 16–41.
- (30) Kuan, S. L., Bergamini, F. R. G., and Weil, T. (2018) Functional protein nanostructures: a chemical toolbox. *Chem. Soc. Rev.* **47**, 9069–9105.
- (31) Sasaki, E., Böhringer, D., van de Waterbeemd, M., Leibundgut, M., Zschoche, R., Heck, A. J. R., Ban, N., and Hilvert, D. (2017) Structure and assembly of scalable porous protein cages. *Nat. Commun.* **8**, 14663.
- (32) Boerakker, M. J., Hannink, J. M., Bomans, P. H. H., Frederik, P. M., Nolte, R. J. M., Meijer, E. M., and Sommerdijk, N. A. J. M. (2002) Giant amphiphiles by cofactor reconstitution. *Angew. Chem., Int. Ed.* **41**, 4239–4241.
- (33) van Dongen, S. F. M., Nallani, M., Cornelissen, J. J. L., Nolte, R. J. M., and van Hest, J. C. M. (2009) A three-enzyme cascade reaction through positional assembly of enzymes in a polymersome nanoreactor. *Chem. - Eur. J.* **15**, 1107–1114.
- (34) Lai, Y. T., Tsai, K. L., Sawaya, M. R., Asturias, F. J., and Yeates, T. O. (2013) Structure and flexibility of nanoscale protein cages designed by symmetric self-assembly. *J. Am. Chem. Soc.* **135**, 7738–7743.
- (35) Lai, Y. T., Reading, E., Hura, G. L., Tsai, K.-L., Laganowsky, A., Asturias, F. J., Tainer, J. A., Robinson, C. V., and Yeates, T. O. (2014) Structure of a designed protein cage that self-assembles into a highly porous cube. *Nat. Chem.* **6**, 1065–1071.
- (36) Hsia, Y., Bale, J. B., Gonan, S., Shi, D., Sheffler, W., Fong, K. K., Nattermann, U., Xu, C., Huang, P.-S., Ravichandran, R., et al. (2016) Design of a hyperstable 60-subunit protein icosahedron. *Nature* **535**, 136–139.
- (37) Kawakami, N., Kondo, H., Matsuzawa, Y., Hayasaka, K., Nasu, E., Sasahara, K., Arai, R., and Miyamoto, K. (2018) Design of hollow protein nanoparticles with modifiable interior and exterior surfaces. *Angew. Chem., Int. Ed.* **57**, 12400–12404.
- (38) Olson, A. J., Bricogne, G., and Harrison, S. C. (1983) Structure of tomato busy stunt virus IV. The virus particle at 2.9 Å resolution. *J. Mol. Biol.* **171**, 61–93.
- (39) Hopper, P., Harrison, S. C., and Sauer, R. T. (1984) Structure of tomato bushy stunt virus. V. Coat protein sequence determination and its structural implications. *J. Mol. Biol.* **177**, 701–713.
- (40) Hsu, C., Singh, P., Ochoa, W., Manayani, D. J., Manchester, M., Schneemann, A., and Reddy, V. S. (2006) Characterization of polymorphism displayed by the coat protein mutants of tomato bushy stunt virus. *Virology* **349**, 222–229.
- (41) Matsuura, K., Watanabe, K., Sakurai, K., Matsuzaki, T., and Kimizuka, N. (2010) Self-assembled synthetic viral capsids from a 24-mer viral peptide fragment. *Angew. Chem., Int. Ed.* **49**, 9662–9665.
- (42) Matsuura, K. (2012) Construction of spherical virus-inspired peptide nanoassemblies. *Polym. J.* **44**, 469–474.
- (43) Matsuura, K., Watanabe, K., Matsushita, Y., and Kimizuka, N. (2013) Guest-binding behavior of peptide nanocapsules self-assembled from viral peptide fragments. *Polym. J.* **45**, 529–534.
- (44) Fujita, S., and Matsuura, K. (2014) Inclusion of zinc oxide nanoparticles into virus-like peptide nanocapsules self-assembled from viral  $\beta$ -annulus peptide. *Nanomaterials* **4**, 778–791.
- (45) Matsuura, K., Nakamura, T., Watanabe, K., Noguchi, T., Minamihata, K., Kamiya, N., and Kimizuka, N. (2016) Self-assembly of Ni-NTA-modified  $\beta$ -annulus peptides into artificial viral capsids and encapsulation of His-tagged proteins. *Org. Biomol. Chem.* **14**, 7869–7874.
- (46) Fujita, S., and Matsuura, K. (2016) Encapsulation of CdTe quantum dots into synthetic viral capsids. *Chem. Lett.* **45**, 922–924.
- (47) Nakamura, Y., Inaba, H., and Matsuura, K. (2019) Construction of artificial viral capsids encapsulating short DNAs via disulfide bonds and controlled release of DNAs by reduction. *Chem. Lett.* **48**, 544–546.
- (48) Matsuura, K., Ueno, G., and Fujita, S. (2015) Self-assembled artificial viral capsid decorated with gold nanoparticles. *Polym. J.* **47**, 146–151.
- (49) Fujita, S., and Matsuura, K. (2017) Self-assembled artificial viral capsids bearing coiled-coils at the surface. *Org. Biomol. Chem.* **15**, 5070–5077.
- (50) Nakamura, Y., Yamada, S., Nishikawa, S., and Matsuura, K. (2017) DNA-modified artificial viral capsids self-assembled from DNA-conjugated  $\beta$ -annulus peptide. *J. Pept. Sci.* **23**, 636–643.
- (51) Komatsu, T., Oguro, Y., Teramura, Y., Takeoka, S., Okai, J., Anraku, M., Otagiri, M., and Tsuchida, E. (2004) Physicochemical

characterization of cross-linked human serum albumin dimer and its synthetic heme hybrid as an oxygen carrier. *Biochim. Biophys. Acta, Gen. Subj.* 1675, 21–31.

(52) Kimura, T., Shinohara, R., Böttcher, C., and Komatsu, T. (2015) Core–shell clusters of human haemoglobin A and human serum albumin: artificial O<sub>2</sub>-carriers having various O<sub>2</sub>-affinities. *J. Mater. Chem. B* 3, 6157–6164.

(53) Sato, H., Nakhaei, E., Kawano, T., Murata, M., Kishimura, A., Mori, T., and Katayama, Y. (2018) Ligand-mediated coating of liposomes with human serum albumin. *Langmuir* 34, 2324–2331.